2024 IEEE International Conference on Environment and Electrical Engineering and 2024 IEEE Industrial and Commercial Power Systems Europe (EEEIC / I&CPS Europe) | 979-8-3503-5518-5/24/$31.00 ©2024 IEEE |
DOI: 10.1109/EEEIC/ICPSEUROPE61470.2024.10751571

A Frequency Stability Scheme Based on Dynamic Estimation and Spectral Clustering

1st Gian Paramo
Electrical and Computer Engineering
University of Florida
Gainesville, USA
gparamo@ufl.edu

2nd Arturo Bretas
Electric Grid Security
Sandia National Laboratories
Albuquerque, USA
asbreta@sandia.gov

3rd Sean Meyn
Electrical and Computer Engineering
University of Florida
Gainesville, USA
meyn@ufl.edu

4th Newton Bretas
Electrical and Computer Engineering
University of Sao Paulo
Sao Carlos, Brazil
ngbretas@sc.usp.br

***Abstract*—Modern frequency stability schemes are static and reactive. They are based on fixed settings and they do not consider the dynamic nature of the grid. These schemes operate only after the system enters a critical state. This work proposes a proactive approach based on the particle filter and spectral clustering. Future frequency values are estimated through the particle filter. This makes it possible to generate an optimized response. This optimization includes establishing areas for distributed control using dynamic system data via spectral clustering. The performance of the concept is evaluated via Matlab simulations using IEEE test systems. The results show that the technique proposed was able to stabilize the test system in the aftermath of a disturbance while providing optimized corrective actions.**

***Index Terms*—Dynamic Estimation, PMU, Synchrophasor, Power System Stability, Underfrequency Control, Filters.**

I. Background

A. Motivation and Literature Review

The modern grid is complex and dynamic, yet most protection and control schemes are static: They are based on fixed settings and do not take into consideration dynamic grid conditions [1]. In the context of underfrequency load-shedding (UFLS), fixed thresholds decide whether the scheme operates or not [2]. Operation is normally carried out at the feeder level with little to no feedback [1]. Equally troubling is the process used for developing these UFLS settings. This process involves running a finite number of simulations, which only covers a few of the operating scenarios the system can encounter [3]. These factors lead to two commonly observed issues: delayed operation and overshedding. In other words, corrective actions are taken only after the system has already entered a critical state, and the amount of compensation used is usually higher than necessary [2]. The introduction of intentional delays and operation based on the rate of change of frequency (RoCoF) have added some degree of flexibility to these schemes, however as the grid continues to evolve, the limitations of static schemes are becoming more evident [1], [2].

In order to overcome these challenges, research has proposed the use of adaptive and predictive schemes. The premise is that an adaptive scheme will eliminate the need to develop fixed settings from simulations, and allow the scheme to make decisions based on real-time data [4]. Also, by being able to predict that the system is heading towards an unstable condition, corrective actions can be optimized [5].

Most techniques in literature shame a common foundation, they propose the use of PMUs for gathering real-time measurements, and then processing these measurements as a time series [2], [5]. A variety of methods are used for producing predictions for instance, autoregressive models are used in [6], model predictive control methods are used in [7], linearized power flow equations are used in [8], the output of synchronous condensers is monitored in [9], and polynomial curve-fitting is utilized in [10].

While the solutions discussed in this section have served as inspiration for this work, they have several limitations in common including: Reliance on high PMU reporting rates, centralized architectures, complex decision making algorithms, lack of robustness during highly dynamic events, the derivation of either purely numerical models or strictly physics-based models. Moreover most of these techniques do not explore the impact of uncertainty.

B. Contributions

The work presented in this paper is an extension of previous research on the application of the particle filter (PF) in power system stability. The PF is fed PMU data and generates predictions a few seconds into the future. This allows the algorithm to optimize a response that stabilizes the system [11], [12]. The goal of this work is to address the limitations of the techniques discussed in the previous section, and to bring this solution one step closer to being implementable. With that goal in mind, the focus of this paper is on the integration of a

clustering module used to establish areas of frequency control based on dynamic system conditions.

The rest of this paper is organized as follows: Section II provides information regarding the proposed scheme architecture, spectral clustering, and the optimization algorithms being used. Section III covers the PF and the equations used to calculate load-generation imbalances. Section IV provides an overview of the solution and the sequence of operation. The performance of the proposed solution is then evaluated through case studies in Section V. Finally, closing remarks are provided in Section VI.

II. Clustering and Optimization

A. Distributed Operation

This work is based on a distributed architecture that leverages Phasor Measurement Units (PMU), and other devices capable of supporting synchrophasors to gather real-time data reflecting the state of the system. One of the main benefits of a distributed architecture is that it streamlines the data transfer process by reducing the amount of information sent to processing nodes [13]. Under this configuration PMUs are grouped based on observability, and only selected PMUs communicate with groups other than their own [5].

B. Spectral Clustering

The term *spectral* refers to techniques based on the analysis of eigenvalues. Eigenvalues hold important information related to the characteristics and the relationships between the states of a system [14]. Spectral clustering is a technique that uses eigenvalues and eigenvectors as a means of dimension reduction to increase clustering efficiency [15].

In this work eigenvalues are derived from a Laplacian matrix. Laplacians are widely used in powers systems to formulate admittance matrices. Instead of using admittance values to built the matrix, power flow measurements are used. The use of power flow values instead of admittance parameters provides access to dynamic load-generation data, which is critical for the process of establishing areas [16] . Off-diagonal entries of the Laplacian, or weights w, are derived from power flows as follows:

$$w_{ij} = w_{ji} = \begin{cases} \frac{|P_{ij}|+|P_{ji}|}{2} & \text{if } e_{ij} \in \mathbf{E} \\ 0 & \text{otherwise} \end{cases} \tag{1}$$

where power flows from i to j, and from j to i are represented by P_{ij} and P_{ji} respectively. e represents the *edges*, or power flow connections, that are part of the overall collection of branches E [16]. These weights are then summed to determine the corresponding diagonal entries of the Laplacian.

$$d_i = \sum_{j=1}^{n} w_{ij} \tag{2}$$

d is referred to as the weighted degree of the node, and is equivalent to the sum of the edges connected to the node.

Edge weights and node degrees are arranged in the Laplacian per eq. 3 as follows:

$$[\mathbf{L}] = \begin{cases} d_i & \text{if } i = j \\ -w_{ij} & i \neq j \text{ and } e_{ij} \in \mathbf{E} \\ 0 & \text{otherwise} \end{cases} \tag{3}$$

The Laplacian is then normalized per:

$$\mathbf{L}_N = \mathbf{D}^{-1/2}\mathbf{L}\mathbf{D}^{-1/2} \tag{4}$$

Normalizing the Laplacian adds flexibility to the solution, especially when working with a diverse set of weights in higher dimensions [16].

The next step is referred to as *spectral embedding*, and it consists of using r eigenvectors of $\mathbf{L}_N$ to map the nodes of the system in the r-dimensional Euclidean space $\mathbb{R}^r$. It is in this new space where the clustering takes place. A variety of clustering algorithms can be used for this purpose including *k*-means [16].

In order to ensure the algorithm produces a suitable set of areas, constraints are put in place, this is a process called *constrained spectral clustering* [15]. Two parameters used to optimize the clustering algorithm are now defined.

The first one is the *boundary* of an area. Boundary measures the impact that removing or islanding, a set of nodes will have on the overall system. The boundary is calculated as the sum of the edge weights linking the potential area or set of nodes S, to nodes belonging to other sets.

$$\partial(S) = \sum_{i \in S,\, j \notin S} w_{ij} \tag{5}$$

A large boundary value indicates a highly connected set of nodes, which can lead to a high power flow disruption if removed.

The second parameter is the *volume* of an area. Volume measures the total power flow - both internal and external of an area.

$$\text{vol}(S) = \sum_{i \in S} d_i \tag{6}$$

Mathematically this is defined as the sum of the weighted-degrees of the nodes in set S. Boundary and volume are then used to assess the quality of an area as follows:

$$\phi(S) = \frac{\partial(S)}{\text{vol}(S)} \tag{7}$$

The $\phi(S)$ of an area quantifies the expected external power flow disruption relative to the volume of the area. Low values of $\phi(S)$ indicate that an area's external power flows make up only a small portion of the total power flow of that area. This makes an area with a low $\phi(S)$ a prime candidate for potential islanding since both internal and external power flow disruptions would be expected to be minimal [16].

C. Optimized Response

An objective function is used to guide the clustering process. Eq. 8, aims to minimize the highest $\phi(S)$ value of the clustering arrangement as follows:

$$\rho_G(k) = \min_{\varnothing \neq S_1,\ldots,S_k \subseteq V} \max_{1 \leq i \leq k} (\phi(S_i)) \tag{8}$$

In other words, eq. 8 selects the clustering solution where the highest values of $\phi(S)$ are the lowest. Additional constraints such as the creation of coherent generator groups or the exclusion of selected power lines can be integrated into the objective function as shown in [16].

One of the main advantages of spectral clustering comes through the use of the Cheeger inequality. This inequality streamlines the optimization process by providing a range of suitable solutions. For a case where k = 2 the inequality is as follows:

$$\frac{v_2}{2} \leq \rho_G(2) \leq \sqrt{2v_2} \tag{9}$$

Focusing on a set of solutions offers a significant improvement in terms of efficiency, compared to evaluating solutions from a much larger set [16]. More information about the Cheeger inequality including a generalized derivation for $k \geq 2$ can be found in [15]. Once the areas have been established, a second layer of optimization, in this case a mixed-integer linear programming (MILP) algorithm, is carried out for each area. The MILP algorithm considers the load-generation balance within each area to generate an optimized response. The algorithm below finds a combination of additional capacity from the sources and identifies feeders that can be dropped in order to balance the system [11], [12].

Algorithm 1 Load Balance Optimization

Initialisation:
A = Source capacity available
B = Sensitive loads available to be shed (feeder level)
C = Non-critical loads available to be shed (feeder level)
c_1^T = Cost of source actuation
c_2^T = Cost of shedding sensitive loads
c_3^T = Cost of shedding non-critical loads
b = Calculated load excess

1: **Minimize** J = $c_1^t x + c_2^t y + c_3^t z$
s.t. $Ax + By + Cz \geq b$
2: **Return** Selected agents in A, B, and C

Additional constraints can be added to the MILP process to meet a wide range of performance specifications.

III. Dynamic Predictions and Compensation

A. Particle Filter

The PF is an estimation algorithm that combines Bayesian inference with the Monte Carlo method. A collection of particles are continuously updated and compared to measurements to estimate an underlying probability distribution. This is done by assigning weights to the particles and redistributing them according to their proximity to the measurements. When these particles are assigned weights, the collection of particles becomes a probability distribution. The average of the weighted particles is then used to estimate the location of the object being measured. These ideas are illustrated in figures 1 and 2.

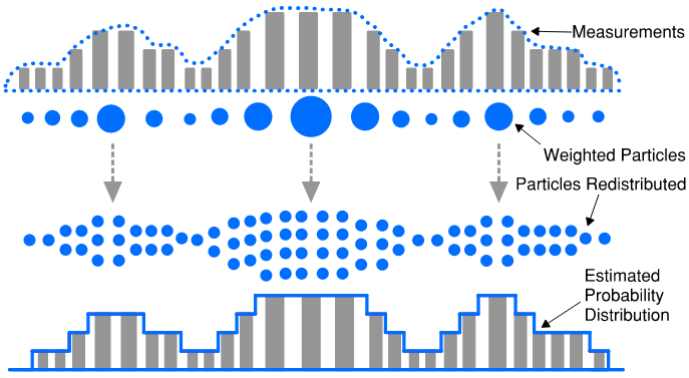

Fig. 1: Estimated Probability Distribution

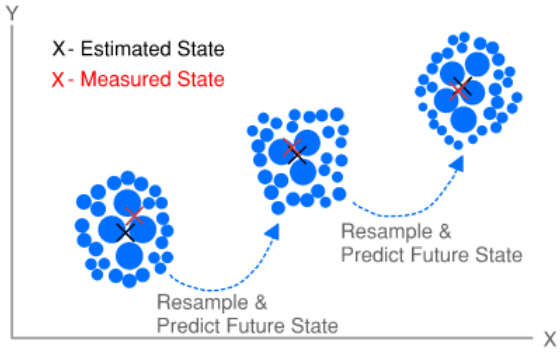

Fig. 2: Particle Based Sampling

A major advantage the PF holds over other popular filters such as the KF, is that the PF is not limited to Gaussian distributions. The use of weighted averages allows the PF to adapt to virtually any probability distribution. This is of particular importance as research has shown that real-life electrical measurements follow a diverse set of probability distributions, beyond the widely assumed Gaussian distribution [11], [12]. Another advantage of the PF is its ability to deliver strong performance in the presence of uncertainty. In many cases uncertainty such as noise, enhances the estimation process [11], [12].

B. Prediction Horizon

Bayesian filters follow a sequential process of predictions and corrections. In general, these predictions have horizons of $k + 1$ steps into the future [11], [12]. In order to perform the calculations presented in this work, these horizons have to be extended. In order to accomplish that, this work uses a variation of the Taylor series to redefine the horizon of the predictions. The first and second derivatives of frequency f, are used to create a vector called Artificial Data Points (ADPs).

$$ADP_i = ADP_{i-1} + tf' + t^2 f'' \tag{10}$$

t is the time window used for the derivatives, this work uses the reporting rates of the measurements as reference. The creation of the ADP vector is a sequential process that starts with the last measurement, ADP_{i-1}, and leverages the first (f') and second (f'') derivatives of frequency to create a trajectory that is later processed by the PF. The number of $ADPs$ needed for a desired horizon can be determined from:

$$N_{ADP} = t_p f_m \tag{11}$$

The number of $ADPs$ required, or N_{ADP}, is a function of the reporting rate of the measurements f_m, measured in frames per second, multiplied by the time horizon of the prediction t_p, measured in seconds [11], [12].

The ADP generation process is summarized as:

Algorithm 2 ADP Generation

Initialisation:
ADP_{i-1} = Last measurement
f' = Average first derivative in last 10 measurements
f'' = Average second derivative in last 10 measurements
N_{ADP} = Number of ADPs required

1: **for** $i = 1$ to N_{ADP} **do**
2: $ADP_i = ADP_{i-1} + t_s f'$
$f' = f' + t_s f''$
3: **end for**

C. Compensation Calculation

When the system is predicted to be entering an unstable condition, calculations are carried out to find the amount of compensation needed to restore stability. The equations used to determine this quantities are derived from the swing equation.

$$L = \frac{R_p H (1 - \frac{f_p^2}{f_1^2})}{pf(f_p - f1)} \tag{12}$$

L represents the excess loading in the system. Power factor is represented by pf. Parameter f is the frequency. Subscript 1 indicates the current frequency value, while subscript p represents the predicted frequency value generated by the PF. R_p is the rate of change of frequency. Subscript p indicates that R is a predicted value. This parameter is found by taking the difference between the current and predicted frequency values and dividing it by the time window t_s as follows:

$$R_p = \frac{f_p - f_1}{t_s} \tag{13}$$

In this work the inertia constant H is assumed to be known, however it can be estimated using the methods described in [11], [12].

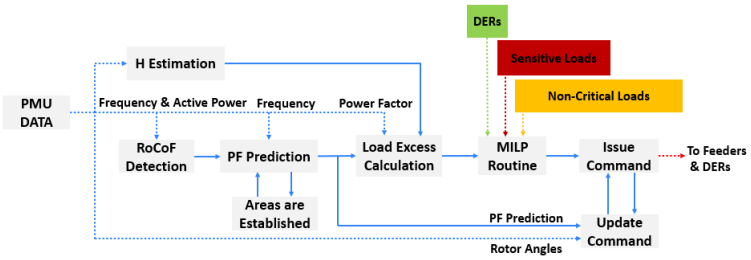

Fig. 3: Solution Overview

TABLE I: Parameters and Initial Conditions (100 MW Base)

Unit No.	H pu	X'd pu	E pu	Angle (rad)
1	500.0	0.006	1.0368	-0.1344
2	30.5	0.0697	1.1966	0.3407
3	35.8	0.0531	1.1491	0.3417
4	38.6	0.0436	1.0808	0.2985
5	26.0	0.132	1.3971	0.5088
6	34.8	0.05	1.1910	0.3376
7	26.4	0.049	1.1394	0.3499
8	24.3	0.057	1.0709	0.3070
9	34.5	0.057	1.1368	0.5335
10	42.0	0.031	1.0929	-0.0087

IV. Scheme Overview

This section provides an overview of the complete scheme and how the different modules complement each other. The process begins when RoCoF thresholds are exceeded. The PF then makes a prediction. If the PF predictions indicate that the system is heading towards an unstable condition, then areas are established. New PF predictions are carried out for each area, and stages of compensation are executed as necessary. These stages of compensation stabilize the system by using the estimated excess loading parameters found with eq. 12, and then identifies a combination of compensation agents through the MILP algorithm. Commands are then sent to the sources and breakers identified by the algorithm. This process is summarized in figure 3.

V. Case Studies

Two case studies are presented in this section. The IEEE 39-Bus test system is used for both cases. Each case starts from the initial conditions shown in Table I. The system is overloaded by 20% over the total generating capacity of the system. This excess loading is split into four equal components and introduced near machines 2, 8, 9, and 7. The Laplacian is calculated from power-flow measurements at least 10 seconds before the disturbances are introduced. Predictions are made 1 second into the future. Noise is added to the PMU measurements, and compensation is carried out 0.5 to 1 seconds after the predictions are made. This is done to account for processing and equipment delays as well as for latency in the communication system.

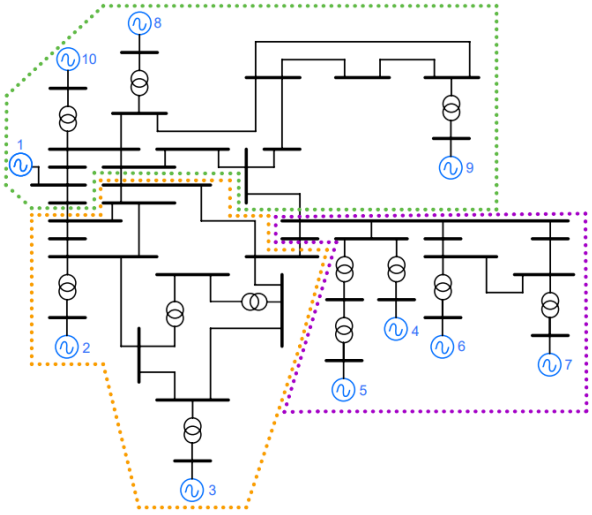

Fig. 4: Three Area Partition

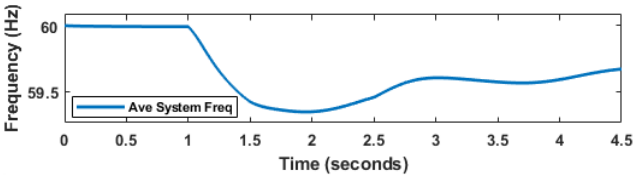

Fig. 5: Complete Frequency Response

A. Case Study I: Three Area Partition

A three area partition is selected for this test scenario. This is illustrated in figure 4. The clustering algorithm identified the areas in less than 0.004 seconds, which is consistent with the results shown in [15] for a system of the same size. The response of the area containing machines 1 and 8-10 is examined. The complete response to the disturbance is displayed in figure 5. After a drop in frequency is identified via the RoCoF method, a prediction is made as illustrated in figure 6. A stage of compensation is carried out at around 1.5 seconds, and shortly after this, a new prediction is made, as illustrated in 7. Since frequency is expected to continue declining a stage of compensation is carried out at around 2 seconds, followed by a new prediction as shown in figure 8. This time, given that the follow-up prediction indicates that frequency will start to return to nominal levels, further stages of compensation are not carried out. The rotor angles of the machines in this area are shown in figure 9.

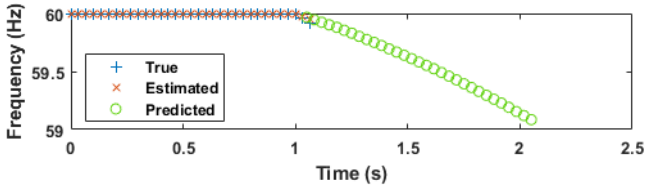

Fig. 6: First Prediction

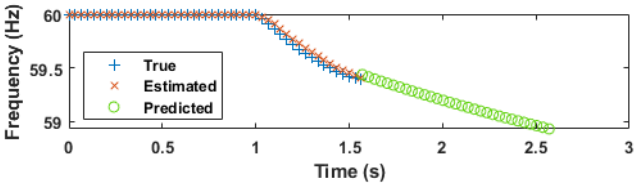

Fig. 7: Second Prediction

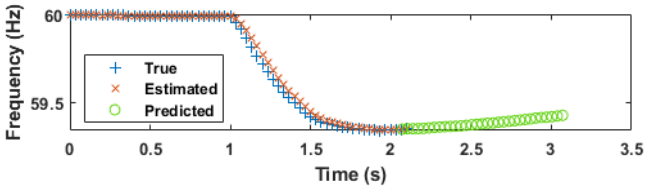

Fig. 8: Third Prediction

B. Case Study II: Four Area Partition

A four area partition is selected for this test scenario as depicted in figure 10. The clustering algorithm found a solution in less than 0.005 seconds, which is consistent with the processing time observed in the first case study and the results in [15]. The response of the area containing machines 1-3 and 10 is examined. The complete response of this area is illustrated in figure 11. The process begins with a prediction at around 1 second per figure 12. The subsequent stage of compensation and the follow-up prediction are shown in figure 13. Since frequency is expected to increase, further compensation is paused until a new decline in frequency is predicted at the 3 second mark as shown in figure 14. This leads to a new stage of compensation at around 3.5 seconds, and a new prediction suggesting that frequency will once again trend back to normal levels. This is illustrated in figure 15. Rotor angles are shown in figure 16.

Additional case studies and comparisons with other techniques can be found in [11] and [12]. In this work the number of areas used for clustering was entered manually, but future work will focus on automating this part of the process.

VI. Conclusion

This paper presented an extension of previous work on predictive frequency stability via PMUs and particle filtering. A spectral clustering module was integrated to the solution to facilitate the process of establishing areas of frequency control. The solution was tested via Matlab simulations and the results

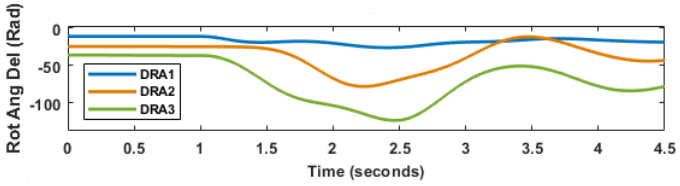

Fig. 9: Rotor Angle Deviations

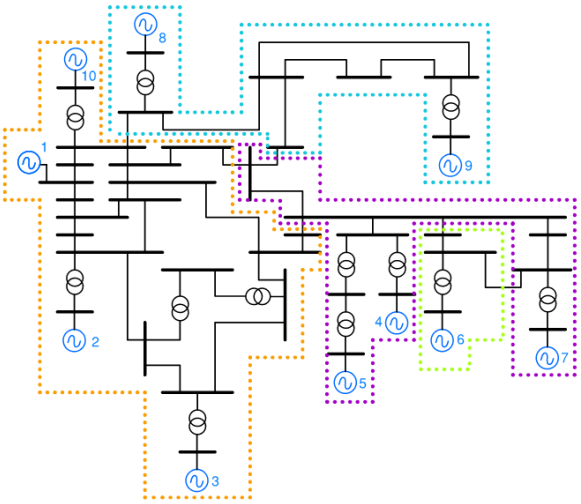

Fig. 10: Four Area Partition

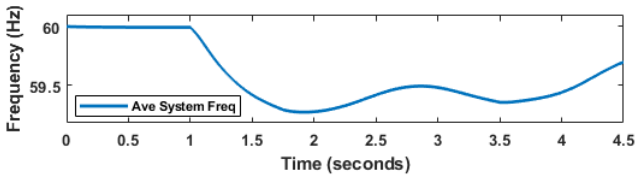

Fig. 11: Complete Frequency Response

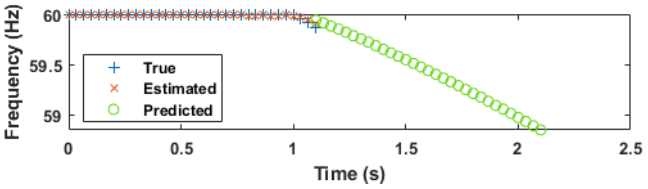

Fig. 12: First Prediction

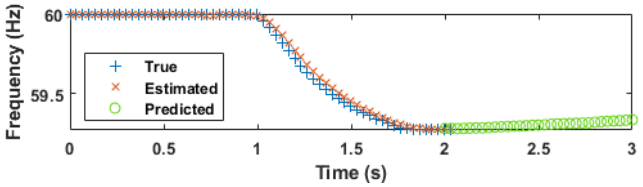

Fig. 13: Second Prediction

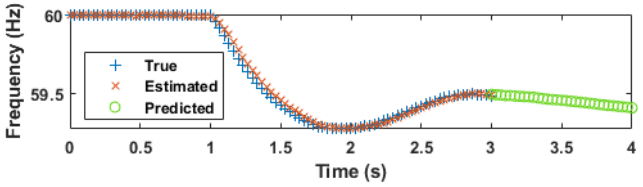

Fig. 14: Third Prediction

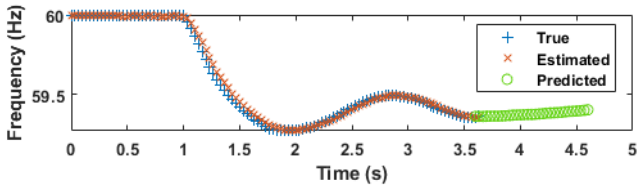

Fig. 15: Fourth Prediction

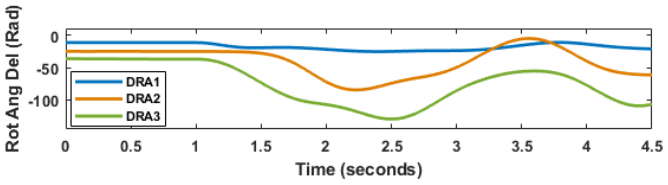

Fig. 16: Rotor Angle Deviations

were satisfactory. Future work will be focused on addressing assumptions made during this process.

REFERENCES

[1] S. H. Horowitz and A. G. Phadke, *Power System Relaying*, 4th, Wiley, West Sussex, United Kingdom, 2014.

[2] L. Sigrist, L. Rouco, and F. M. Echavarren, "A review of the state of the art of UFLS schemes for isolated power systems," in International Journal of Electrical Power & Energy Systems, vol 99, pp. 525–539, 2018, doi: 10.1016/j.ijepes.2018.01.052.

[3] NERC Standards, PRC-006-SERC-02, 2017.

[4] P. M. Anderson and M. Mirheydar, "An adaptive method for setting underfrequency load shedding relays," in IEEE Transactions on Power Systems, vol. 7, no. 2, pp. 647-655, May 1992, doi: 10.1109/59.141770.

[5] G. Paramo, A. Bretas, and S. Meyn, "Research Trends and Applications of PMUs," Energies, vol. 15, no. 15, p. 5329, Jul. 2022, doi: 10.3390/en15155329.

[6] N. G. Bretas, and A. G. Phadke, "Real time instability prediction through adaptive time series coefficients," IEEE Power Engineering Society. 1999 Winter Meeting (Cat. No.99CH36233), 1999, pp. 731-736 vol.1, doi: 10.1109/PESW.1999.747547.

[7] A. Parisio, E. Rikos, and L. Glielmo, "A Model Predictive Control Approach to Microgrid Operation Optimization," in IEEE Transactions on Control Systems Technology, vol. 22, no. 5, pp. 1813-1827, Sept. 2014, doi: 10.1109/TCST.2013.2295737.

[8] M. Larsson, and C. Rehtanz, "Predictive frequency stability control based on wide-area phasor measurements," IEEE Power Engineering Society Summer Meeting,, 2002, pp. 233-238 vol.1, doi: 10.1109/PESS.2002.1043222.

[9] A. Sauhats, A. Utans, J. Silinevics, G. Junghans, and D. Guzs, "Enhancing Power System Frequency with a Novel Load Shedding Method Including Monitoring of Synchronous Condensers' Power Injections," Energies, vol. 14, no. 5, p. 1490, Mar. 2021, doi: 10.3390/en14051490.

[10] U. Rudez, and R. Mihalic, "WAMS-Based Underfrequency Load Shedding With Short-Term Frequency Prediction," in IEEE Transactions on Power Delivery, vol. 31, no. 4, pp. 1912-1920, Aug. 2016, doi: 10.1109/TPWRD.2015.2503734.

[11] G. Paramo, and A. Bretas, "Proactive Frequency Stability Scheme: A Distributed Framework Based on Particle Filters and Synchrophasors," Energies, vol. 16, no. 11, p. 4530, Jun. 2023, doi: 10.3390/en16114530.

[12] G. Paramo, and A. Bretas, "Proactive Frequency Stability Scheme via Bayesian Filters and Synchrophasors," 2023 IEEE Kansas Power and Energy Conference (KPEC), Manhattan, KS, USA, 2023, pp. 1-6, doi: 10.1109/KPEC58008.2023.10215435.

[13] A. Chakrabortty and P. P. Khargonekar, "Introduction to wide-area control of power systems," 2013 American Control Conference, Washington, DC, USA, 2013, pp. 6758-6770, doi: 10.1109/ACC.2013.6580901.

[14] G. Paramo, A. Bretas and S. Meyn, "High-Impedance Non-Linear Fault Detection via Eigenvalue Analysis with low PMU Sampling Rates," 2023 IEEE Power & Energy Society Innovative Smart Grid Technologies Conference (ISGT), Washington, DC, USA, 2023, pp. 1-5, doi: 10.1109/ISGT51731.2023.10066424.

[15] J. Quirós-Tortós, R. Sánchez-García, J. Brodzki, J. Bialek, and V. Terzija, "Constrained spectral clustering-based methodology for intentional controlled islanding of large-scale power systems," in IET Gener. Transm. Distrib., vol. 9, pp. 31-42, 2015, doi: doi.org/10.1049/iet-gtd.2014.0228.

[16] R. J. Sánchez-García et al., "Hierarchical Spectral Clustering of Power Grids," in IEEE Transactions on Power Systems, vol. 29, no. 5, pp. 2229-2237, Sept. 2014, doi: 10.1109/TPWRS.2014.2306756.

[17] P. Brunelle, "10-Machine New-England Power System IEEE Benchmark", MATLAB Central File Exchange, 2023, https://www.mathworks.com/matlabcentral/fileexchange/54771-10-machine-new-england-power-system-ieee-benchmark.